



## Comparison of experimental and theoretical GaInP quantum well gain spectra

W. W. Chow, P. M. Snowton, P. Blood, A. Girndt, F. Jahnke, and S. W. Koch

Citation: [Applied Physics Letters](#) **71**, 157 (1997); doi: 10.1063/1.119489

View online: <http://dx.doi.org/10.1063/1.119489>

View Table of Contents: <http://scitation.aip.org/content/aip/journal/apl/71/2?ver=pdfcov>

Published by the [AIP Publishing](#)

---



## Re-register for Table of Content Alerts

Create a profile.



Sign up today!



# Comparison of experimental and theoretical GaInP quantum well gain spectra

W. W. Chow<sup>a)</sup>

Sandia National Laboratories, Albuquerque, New Mexico 85718-0601

P. M. Smowton and P. Blood

Department of Physics and Astronomy, University of Wales, Cardiff, Cardiff CF2 3YB, United Kingdom

A. Girndt, F. Jahnke, and S. W. Koch

Department of Physics and Material Sciences Center, Philipps University, Renthof 5, 35032 Marburg, Germany

(Received 25 March 1997; accepted for publication 13 May 1997)

A microscopic analysis of experimental GaInP quantum well gain spectra is presented for a wide range of excitation. A consistent treatment of carrier collision effects, at the level of quantum kinetic theory in the Markovian limit, is found to be necessary for agreement with experiment. © 1997 American Institute of Physics. [S0003-6951(97)02928-8]

To design 620–690 nm GaInP quantum well lasers for an expanding range of applications, it is necessary to be able to predict their gain spectra accurately. For example, the wavelength and temperature dependences of threshold current in a vertical-cavity surface-emitting laser are strongly affected by the shape and density dependence of the gain spectrum. Although there have been some reports of the less demanding task of fitting gain versus current curves,<sup>1</sup> and some experimental measurements of gain spectra,<sup>2</sup> as yet there has been little success in matching experimental gain spectra with theoretical calculations.

We have measured spontaneous emission through a 4- $\mu\text{m}$ -wide opening in the top contact of 50- $\mu\text{m}$ -wide oxide stripe lasers, fabricated from material containing 6.8-nm-wide, compressively strained Ga<sub>0.41</sub>In<sub>0.59</sub>P quantum wells set in an (Al<sub>0.5</sub>Ga<sub>0.5</sub>)<sub>0.51</sub>In<sub>0.49</sub>P waveguide core and cladded with (Al<sub>0.7</sub>Ga<sub>0.3</sub>)<sub>0.51</sub>In<sub>0.49</sub>P. By measurement of the wavelength of the laser line and the slope of the spontaneous emission spectrum, we were able to determine the quasi-Fermi level separation at threshold.<sup>3</sup> This information is used in the relationship between gain and spontaneous emission<sup>4</sup> to determine the gain spectrum. The points in Fig. 1 show the spectra measured from the same sample at injection currents of 100, 140 and 180 mA.

When calculating semiconductor laser gain spectra, one often approximates collision effects with an effective dephasing rate,  $\gamma$ .<sup>5</sup> Such an approach yields the formula for the intensity gain (mks units)<sup>6,7</sup>

$$G = \frac{\omega}{\epsilon_0 n c \hbar \gamma V} \sum_{\nu_e, \nu_h} \sum_{\mathbf{k}} |\mu_{\mathbf{k}}^{\nu_e, \nu_h}|^2 (n_{\mathbf{k}}^{\nu_e} + n_{\mathbf{k}}^{\nu_h} - 1) \times L(\omega - \omega_{\mathbf{k}}^{\nu_e, \nu_h}) \text{Re}(Q_{\mathbf{k}}^{\nu_e, \nu_h}), \quad (1)$$

where  $n_{\mathbf{k}}^{\nu_e(\nu_h)}$  is the electron (hole) population in quantum well subband  $\nu_e(\nu_h)$  and momentum  $\mathbf{k}$ ,  $\omega_{\mathbf{k}}^{\nu_e, \nu_h}$  is the transition frequency,  $\omega$  is the laser frequency,  $\epsilon_0$  and  $c$  are the permittivity and speed of light in vacuum,  $n$  is the back-

ground refractive index,  $V$  is the active region volume, and  $\mu_{\mathbf{k}}^{\nu_e, \nu_h}$  is the optical transition dipole matrix element. The line shape function,  $L(\omega - \omega_{\mathbf{k}}^{\nu_e, \nu_h})$  which accounts for polarization dephasing effects, is usually assumed to be a Lorentzian,  $L(x) = [1 + (x/\gamma)^2]^{-1}$ , where the dephasing rate,  $\gamma$  is an input parameter in the gain calculation. In the above equation, the many-body Coulomb effects are treated at the level of the Hartree–Fock approximation.<sup>6,7</sup> They give rise to a carrier density dependence in the transition energy,  $\omega_{\mathbf{k}}^{\nu_e, \nu_h}(N)$ , and a renormalization of the Rabi frequency, which leads to the excitonic or Coulomb enhancement factor,  $Q_{\mathbf{k}}^{\nu_e, \nu_h}(N)$ . While Eq. (1) has been successful in explaining some experimental data,<sup>8–10</sup> the phenomenological treatment of carrier collision effects appears inadequate for reproducing certain important spectral features. The curves in Fig. 1

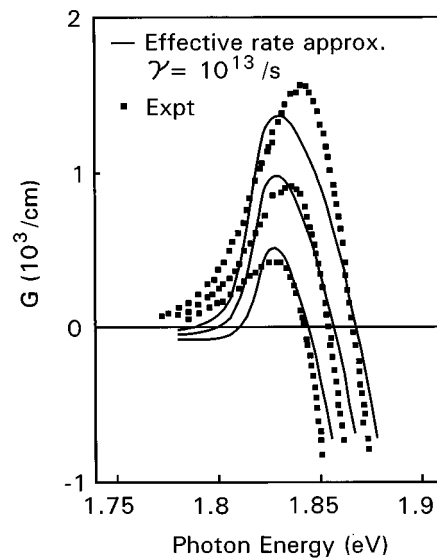


FIG. 1. Gain spectra for a 6.8 nm Ga<sub>0.41</sub>In<sub>0.59</sub>P/(Al<sub>0.5</sub>Ga<sub>0.5</sub>)<sub>0.51</sub>In<sub>0.49</sub>P quantum well. The points are from experiment at injection currents,  $I=100$ , 140 and 180 mA. The curves are calculated using Eq. (1), with dephasing rate,  $\gamma=10^{13} \text{ s}^{-1}$  and carrier densities,  $N=2.6 \times, 3.0 \times, 3.4 \times 10^{12} \text{ cm}^{-2}$  chosen to give the best fit to the experimental spectra.

<sup>a)</sup>Electronic mail: wwchow@somnet.sandia.gov

are obtained using Eq. (1), with dephasing rate and carrier densities chosen to best fit the experimental data. The calculated spectra show an unphysical absorption below the band gap energy, a considerably steeper rise in gain from the band edge than experiment, and negligible shift in the gain peak with excitation. Based on the argument of non-Markovian response, line shape functions besides the Lorentzian have been proposed.<sup>11,12</sup> However, they remain unsatisfactory in terms of accurately describing the gain in the neighborhood of the band edge, the general shape of the quantum well gain spectrum, and the spectral changes with changing carrier density. Equally important is the limitation to predictive capability because of the need to treat the dephasing rate as an input parameter.

This letter describes the results of a more detailed treatment of collision effects in a semiconductor gain medium, that involves extending the screened Hartree–Fock treatment to include contributions from the next higher order correlations involving the Coulomb potential. The resulting equation of motion for the microscopic polarization due to an electron-hole pair,  $p_{\mathbf{k}}^{v_e, v_h}$  has the form,<sup>13–15</sup>

$$\begin{aligned} \frac{d}{dt} p_{\mathbf{k}}^{v_e, v_h} = & -i\omega_{\mathbf{k}}^{v_e, v_h} p_{\mathbf{k}}^{v_e, v_h} - i\Omega_{\mathbf{k}}^{v_e, v_h} (n_{\mathbf{k}}^{v_e} + n_{\mathbf{k}}^{v_h} - 1) \\ & - (\Gamma_{\mathbf{k}}^{v_e} + \Gamma_{\mathbf{k}}^{v_h}) p_{\mathbf{k}}^{v_e, v_h} + \sum_q (\Gamma_{\mathbf{k}, \mathbf{q}}^{v_e} + \Gamma_{\mathbf{k}, \mathbf{q}}^{v_h}) p_{\mathbf{k}+\mathbf{q}}^{v_e, v_h}. \end{aligned} \quad (2)$$

The first two terms on the right hand side describe the oscillation of the polarization at the transition frequency,  $\omega_{\mathbf{k}}^{v_e, v_h}$ , and the stimulated emission and absorption processes. The screened Hartree–Fock contributions lead to a band gap renormalization, resulting in a transition energy,

$$\begin{aligned} \hbar\omega_{\mathbf{k}}^{v_e, v_h}(N) = & \varepsilon_{\mathbf{k}}^{v_e} + \varepsilon_{\mathbf{k}}^{v_h} + [\varepsilon_{g,0} + \Delta\varepsilon_{CH}^{v_e, v_h}(N) \\ & + \Delta\varepsilon_{SX}^{v_e, v_h}(N)], \end{aligned} \quad (3)$$

where  $\varepsilon_{\mathbf{k}}^{v_e(v_h)}$  is the single-particle electron (hole) energy,  $\Delta\varepsilon_{CH}^{v_e, v_h}$  and  $\Delta\varepsilon_{SX}^{v_e, v_h}$  are the Coulomb hole and exchange contributions, respectively. They also result in the renormalization of the Rabi frequency

$$\Omega_{\mathbf{k}}^{v_e, v_h} = \frac{1}{\hbar} \left( \mu_{\mathbf{k}}^{v_e, v_h} E + \sum_q V_{s,q} p_{\mathbf{k}+\mathbf{q}}^{v_e, v_h} \right), \quad (4)$$

where the Fourier transform of the screened Coulomb potential energy,  $V_{s,q}$ , contains integrals involving the bounded quantum well eigenfunctions, to account for the effects of finite quantum well width and confinement potential. Carrier–carrier collisions give rise to the last two terms.<sup>14,15</sup> The third term in Eq. (2) is a diagonal contribution, with

$$\begin{aligned} \Gamma_{\mathbf{k}}^{v_e} = & \sum_{v', v'', v'''} \sum_{\mathbf{q}, \mathbf{k}'} \frac{2\pi}{\hbar} V_{s,q}^2 \delta(\varepsilon_{\mathbf{k}}^{v_e} + \varepsilon_{\mathbf{k}'}^{v''} - \varepsilon_{\mathbf{k}+\mathbf{q}}^{v'} - \varepsilon_{\mathbf{k}'-\mathbf{q}}^{v'''}) \\ & \times [n_{\mathbf{k}+\mathbf{q}}^{v'} (1 - n_{\mathbf{k}'}^{v''}) n_{\mathbf{k}'-\mathbf{q}}^{v'''} + (1 - n_{\mathbf{k}+\mathbf{q}}^{v'}) n_{\mathbf{k}'}^{v''} (1 \\ & - n_{\mathbf{k}'-\mathbf{q}}^{v'''})]. \end{aligned} \quad (5)$$

The fourth term is a nondiagonal contribution, which couples polarizations with different  $\mathbf{k}$ s. For this contribution,

$$\begin{aligned} \Gamma_{\mathbf{k}, \mathbf{q}}^{v_e} = & \sum_{v', v'', v'''} \sum_{\mathbf{k}'} \frac{2\pi}{\hbar} V_{s,q}^2 \delta(\varepsilon_{\mathbf{k}}^{v_e} + \varepsilon_{\mathbf{k}'}^{v''} - \varepsilon_{\mathbf{k}+\mathbf{q}}^{v'} - \varepsilon_{\mathbf{k}'-\mathbf{q}}^{v'''}) \\ & \times [(1 - n_{\mathbf{k}}^{v_e}) (1 - n_{\mathbf{k}'}^{v''}) n_{\mathbf{k}'-\mathbf{q}}^{v'''} \\ & + n_{\mathbf{k}}^{v_e} n_{\mathbf{k}'}^{v''} (1 - n_{\mathbf{k}'-\mathbf{q}}^{v'''})]. \end{aligned} \quad (6)$$

In this letter, screening effects are treated with the screened Coulomb potential energy,  $V_{s,q}$ , which is obtained by using the Lindhard formula for the static longitudinal dielectric function.<sup>6,7</sup> Doing so reduces numerical complexity because it eliminates one nested integral from the collision terms. A more consistent approach involves staying with the bare (unscreened) Coulomb potential throughout the derivation of Eq. (2). In this case, the Hartree–Fock contributions are given in terms of the unscreened Coulomb potential, and the leading screening contributions appear as the principal (and imaginary) part of the Coulomb correlation terms.<sup>16</sup> Comparison with the principal value results for a few selected densities show our short cut to be quite accurate for the experimental conditions treated in this letter. Finally, from semiclassical laser theory and Maxwell's equations, we get (mks units)<sup>7</sup>

$$\begin{aligned} \frac{dE}{dz} = & \frac{G}{2} E \\ = & - \frac{\omega}{\varepsilon_0 n c V} \text{Im} \left( \sum_{v_e, v_h} \sum_{\mathbf{k}} (\mu_{\mathbf{k}}^{v_e, v_h})^* p_{\mathbf{k}}^{v_e, v_h} e^{i\omega t} \right), \end{aligned} \quad (7)$$

where  $E$  is the slowly varying electric field amplitude. To evaluate the small signal gain, we assume a weak laser field and quasiequilibrium carrier distributions. The weak laser field allows us to neglect the changes in the carrier densities (linear response), so that one has to numerically solve only Eq. (2) for the steady state polarizations,  $p_{\mathbf{k}}^{v_e, v_h}$ . Substituting the result in Eq. (7) and performing the sums over carrier momenta and quantum well subbands give the gain.

The curves in Fig. 2 show the calculated spectra. We assume parabolic conduction subbands, with band edge energies determined by the bound states energies of the quantum well. To determine the hole energy dispersions, we use a 6×6 Luttinger–Kohn Hamiltonian and the envelope approximation. Input parameters to the band structure calculations are the bulk material Luttinger parameters,<sup>17</sup> unrenormalized band gap energies and offsets,<sup>18</sup> deformation potentials and lattice constants.<sup>17,19</sup> The band structure calculation also gives the dipole transition elements. We chose the densities so that the theoretical and experimental quasiequilibrium chemical potential separations coincide. The use of the chemical potential separation circumvents the need to convert from carrier density to current density, which requires knowledge of carrier recombination (radiative and nonradiative) rates. Figure 2 shows that the theory reproduces the experimental data very well, especially the gradual bulklike rise in gain with increasing photon energy, and the blue shift in the gain peak with increasing excitation. Figure 3 shows that the agreement extends over a wide range of excitation.

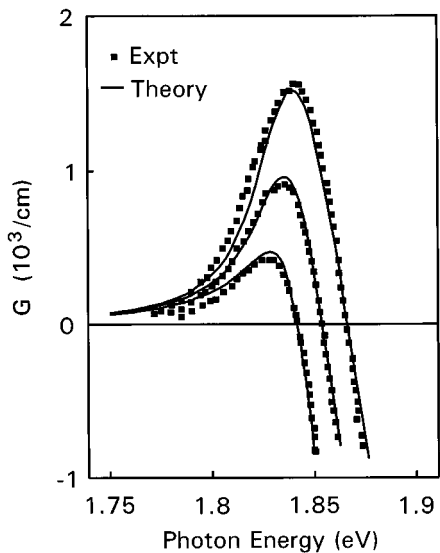


FIG. 2. Gain spectra for a 6.8 nm  $\text{Ga}_{0.41}\text{In}_{0.59}\text{P}/(\text{Al}_{0.5}\text{Ga}_{0.5})_{0.51}\text{In}_{0.49}\text{P}$  quantum well. The points are from experiment and the curves are calculated by numerically solving the polarization equation of motion, Eq. (2), and using Eq. (7). The carrier densities are  $N=2.2\times, 2.7\times, 3.2\times 10^{12} \text{ cm}^{-2}$ .

Plotted are the peak gain and gain peak energy versus chemical potential separation. The solid points are from the experimental spectra shown in Figs. 1 and 2, while the unfilled points are from additional experimental data that span a wider excitation range. The dashed curves are obtained using the effective rate approximation, Eq. (1). The results show

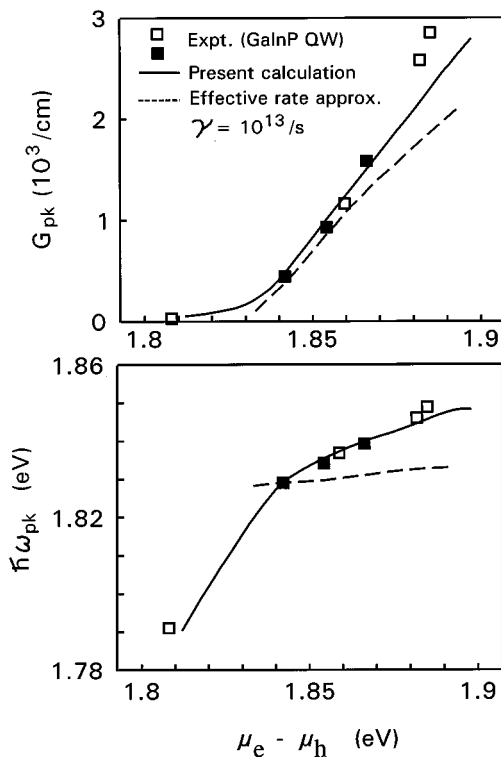


FIG. 3. (Top) peak gain and (bottom) gain peak frequency vs chemical potential separation. The solid curves are obtained using our approach, and the dashed curves are obtained using the effective rate approximation, with  $\gamma=10^{13} \text{ s}^{-1}$ . The points are from experiment, with the solid points corresponding to the experimental spectra shown in Figs. 1 and 2.

that the more detailed treatment of Coulomb collision effects is crucial, especially at low excitations, or when the accurate location of the gain peak is desired. Finally, our calculations give an exciton energy of 14 meV for the quantum well structure considered. This value falls within the range of 11–15 meV measured in experiments.<sup>18</sup>

In summary, we obtained good agreement, over a wide excitation range, between experiment and theory for the gain spectra of InGaP quantum wells. The calculations are based on the Semiconductor Bloch Equations, with carrier collision effects treated at the level of quantum kinetic theory in the Markovian limit. This approach gives a consistent description of collision effects, which give rise to both diagonal and nondiagonal Coulomb correlations. Calculations based on the effective rate approximation take into account only the diagonal effects, and as a result do not accurately describe several important features of the experimental spectrum. Besides resulting in better agreement with experiment, our approach improves predictive capability by eliminating the use of the dephasing rate as an input parameter.

This work was supported in parts by the U.S. Department of Energy under Contract No. DE-AC04-94AL85000, the Engineering and Physical Sciences Research Council (U.K.), the Deutsche Forschungsgemeinschaft (Germany), the Leibniz Prize, and AFOSR-F49620-97-1-0002.

- <sup>1</sup>H. D. Summers, P. Blood, and P. Rees, *Appl. Phys. Lett.* **63**, 2792 (1993).
- <sup>2</sup>G. Hunziker, W. Knop, P. Unger, and C. Harder, *IEEE J. Quantum Electron.* **31**, 643 (1995).
- <sup>3</sup>P. Blood, A. I. Kucharska, J. P. Jacobs, and K. Griffiths, *J. Appl. Phys.* **70**, 1144 (1991).
- <sup>4</sup>C. H. Henry, R. A. Logan, and F. R. Merritt, *J. Appl. Phys.* **51**, 3042 (1980).
- <sup>5</sup>M. Yamada and Y. Suematsu, *J. Appl. Phys.* **52**, 2653 (1981).
- <sup>6</sup>H. Haug and S. W. Koch, *Quantum Theory of the Optical and Electronic Properties of Semiconductors*, 3rd ed. (World Scientific, Singapore, 1994).
- <sup>7</sup>W. W. Chow, S. W. Koch, and M. Sargent III, *Semiconductor-Laser Physics* (Springer, Berlin, 1994).
- <sup>8</sup>R. Jin, D. Boggavarapu, G. Khitrova, H. M. Gibbs, Y. Z. Hu, S. W. Koch, and N. Peyghambarian, *Appl. Phys. Lett.* **61**, 1883 (1992).
- <sup>9</sup>Y. H. Lee, A. Chavez-Pirson, S. W. Koch, H. M. Gibbs, S. H. Park, J. Morhange, A. Jeffery, N. Peyghambarian, L. Banyai, A. C. Gossard, and W. Wiegmann, *Phys. Rev. Lett.* **57**, 2446 (1986).
- <sup>10</sup>W. W. Chow, S. W. Corzine, D. B. Young, and L. A. Coldren, *Appl. Phys. Lett.* **66**, 2460 (1995).
- <sup>11</sup>M. Yamamishi and Y. Lee, *IEEE J. Quantum Electron.* **23**, 367 (1987).
- <sup>12</sup>D. Ahn, *IEEE J. Quantum Electron.* **32**, 960 (1996).
- <sup>13</sup>M. Lindberg and S. W. Koch, *Phys. Rev. B* **38**, 3342 (1988).
- <sup>14</sup>F. Jahnke, M. Kira, S. W. Koch, G. Khitrova, E. K. Lindmark, T. R. Nelson, Jr., D. V. Wick, J. D. Berger, O. Lyngnes, H. M. Gibbs, and K. Tai, *Phys. Rev. Lett.* **77**, 5257 (1996).
- <sup>15</sup>W. W. Chow, A. Knorr, S. Hughes, A. Girndt, and S. W. Koch, *IEEE J. Sel. Topics Quantum Electron.* (to be published).
- <sup>16</sup>T. Rappen, U-G Peter, M. Wegener, and W. Schäfer, *Phys. Rev. B* **49**, 10774 (1994), and references cited therein.
- <sup>17</sup>O. Madelung, *Landolt-Bornstein Numerical Data and Functional Relationships in Science and Technology* (Springer, Berlin, 1982), Vol. 17a.
- <sup>18</sup>M. D. Dawson and G. Duggan, *Phys. Rev. B* **47**, 12598 (1993).
- <sup>19</sup>S. Adachi, *Physical Properties of III-V Semiconductor Compounds* (Wiley, New York, 1992).